ELSEVIER

Catalysis Today 85 (2003) 31–37

CATALYSIS TODAY

www.elsevier.com/locate/cattod

Reduction of NO by CO on Pt-MoO_3/γ-Al_2O_3 catalysts

Mônica Antunes Pereira da Silva [a], Martin Schmal [a,b,*]

[a] *Escola de Química/UFRJ, Ilha do Fundão, C.P. 68542, 21949-900 Rio de Janeiro, Brazil*
[b] *NUCAT/PEQ/COPPE/UFRJ, C.P. 68502, 21945-970 Rio de Janeiro, Brazil*

Abstract

This work is concerned with the interaction between platinum and molybdenum oxide for Pt-MoO_3/γ-Al_2O_3 catalysts. Two types of characterization techniques were used: thermal analysis; and NO and H_2 desorption at programmed temperature. The results of thermal analysis as well as those of hydrogen desorption suggest bronze formation for catalysts with Mo. The NO desorption data show that Mo is the main responsible for the N_2 selectivity. The activity of the catalysts was evaluated with reduction of nitric oxide by carbon monoxide. A synergic behavior was observed between Pt and Mo. Product selectivity of the NO reduction by CO is function of the prevailing treatment and reaction conditions and suggests significant changes of surface sites during the reaction.

Keywords: Reduction of NO; NO TPD; Characterization of Pt-MoO_3/γ-Al_2O_3

1. Introduction

Intensive research aiming to reduce air pollution caused by automotive exhaust gases has been done in the last years. The catalytic NO reduction was investigated deeply in connection with a number of practical applications in enclosed environments, odor control and volatile organic compounds. It has been shown early that noble metals, platinum, rhodium and palladium in particular, are the most active for promoting reductive reactions Therefore, a large effort has been made focusing this reaction based on catalysts containing these elements [1–3]. The noble metals are responsible for the elimination of CO, hydrocarbons and the reduction of NO_x from exhausted gases. Several studies were reported aiming to diminish the Rh contents and also to eliminate them by substituting with other less expensive elements or rare transition metals. One alternative is the association of molybdenum oxide with a noble metal (Pt or Pd) [1–3].

Molybdenum plays an important role in the stabilization of the active metal and the alumina support, by enhancing the oxygen storage capacity and spillover effect. The surface migration is quite important in oxidation reactions, since the catalysts are submitted to reduction–oxidation cycles. Moreover, the metal–oxide combination may affect strongly the oxygen mobility by chemical metal–support interaction [4]. However, the presence of the spillover and bronze formation in oxi-reduction catalysis need to be explored in greater depth.

The objective of this work was to study the effect of molybdenum loading and the interaction between platinum and molybdenum oxide supported on γ-alumina. Characterization techniques, such as thermal analysis and temperature programmed desorption of H_2 and NO were used for this purpose. The catalytic activity was evaluated with the reduction of NO by CO.

* Corresponding author. Fax: +55-21-2290-6626.
E-mail addresses: monica@eq.ufrj.br (M.A.P. da Silva), schmal@peq.coppe.ufrj.br (M. Schmal).

0920-5861/$ – see front matter © 2003 Elsevier B.V. All rights reserved.
doi:10.1016/S0920-5861(03)00191-3

2. Experimental

2.1. Preparation of catalysts

The catalysts Pt-MoO_3/γ-Al_2O_3 were prepared using wet impregnation, as described elsewhere [4–6]. Prepared catalysts will be referred as *x*Pt-*y*Mo, where *x* (1%) and *y* (2–20%) represent the weight percentage of Pt and Mo, respectively.

2.2. Characterization

Thermal analysis was performed in a thermobalance Rigaku TG 8110. The gas flow was a mixture of 30 cm^3/min of N_2 and 10 cm^3/min of H_2. The temperature was raised at 10 °C/min up to 1473 K. The reference material was α-Al_2O_3.

The TPD equipment was coupled to a quadrupole mass spectrometer (Balzers, PRISMA-QMS 200) equipped with a acquisition data system. Initially, the catalyst was dried at 423 K for 60 min (10 K/min), under He flow at 30 cm^3/min. After cooling to room temperature, the catalyst was reduced with pure H_2 (60 cm^3/min) at 773 K for 2 h (10 K/min), then purged with He for 30 min at 773 K and cooled to room temperature to eliminate H_2. The adsorption of NO was carried out at room temperature under 1%NO/He flow for 30 min. The temperature was raised up to 823 K at 20 K/min and held for 1 h. In the case of H_2 TPD, adsorption was accomplished by frontal method. During TPD the reactor was heated up to 773 K under similar conditions as before.

The reduction of NO by CO (ratio CO/NO = 1.67) was carried out in a microreactor with space velocity 70,000 h^{-1}. Samples were priori dried and reduced with pure H_2 (30 cm^3/min) at 773 K for 2 h, and then purged with He at this temperature for 30 min. Catalytic tests were performed at 573 K and the effect of water was evaluated passing water vapor (10% molar) from saturator in the feed mixture.

3. Results and discussion

3.1. Analyses of TG/DTA

Fig. 1 displays the loss of mass with temperature during thermogravimetric analyses.

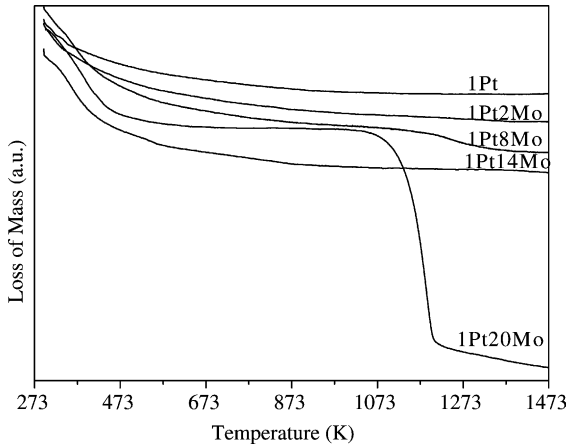

Fig. 1. Thermogravimetric analysis of calcined catalysts.

The results are related to the reduction of platinum and molybdenum oxide. The loss of mass between 573 and 853 K was negligible. For high Mo loading catalysts the reduction is easy. It suggests that the loss of mass associated to the reduction is compensated by the formation of hydrogen bronzes species (H_xMoO_3) [4,7]. The significant weight loss for the 1Pt20Mo catalyst between 1073 and 1273 K is attributed to molybdenum volatilization [3].

Fig. 2 presents the profiles of differential thermal analysis. With exception of 1Pt20Mo, all catalysts presented one endothermic peak around 320 K, which was associated to the loss of humidity. However, the 1Pt20Mo catalyst presented a broad exothermic peak

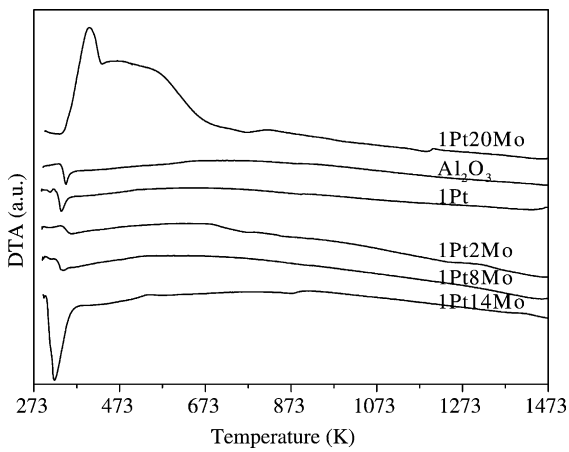

Fig. 2. Differential thermal analysis of calcined catalysts.

with maximum well defined at 404 K, which can be associated to bronze species formation (H_xMoO_3). In addition, TGA curves showed the compensation of weight loss due to bronze formation with increasing Mo content. The second peak above 473 K is associated to reduction of Mo oxide. Indeed, TPR profiles confirmed the transformation of Mo^{6+} to Mo^{4+} occurring at higher temperatures and the corresponding transformations and explanations were reported previously [6]. Notice that the concentration of H_2 in the mixture for TPR analysis [6] was different from the present TGA/DTA experiment, which explains the peak shift displayed here. Moreover, we observed, in agreement with our previous report [4], that there is a different environment around Mo species for higher Mo contents.

3.2. Hydrogen temperature programmed desorption (H_2 TPD)

Fig. 3 displays the TPD spectra of H_2 for the catalysts reduced at 773 K.

Catalyst 1Pt exhibits three H_2 desorption peaks at 455, 707 and 773 K.

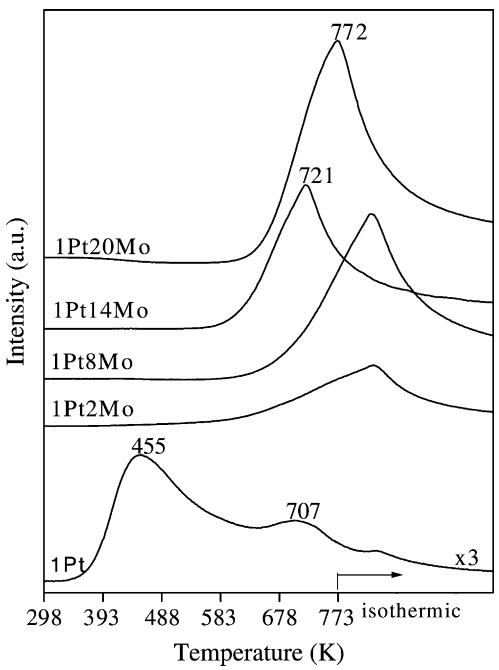

Fig. 3. TPD spectra for H_2 adsorbed on catalysts reduced at 773 K.

H_2 TPD on Pt/zeolite displays also three H_2 desorption peaks [8–10]. The first one at low temperature (ca. 423 K) is due to the hydrogen chemisorption on the metal surface. At higher temperatures (473–773 K), these peaks can be assigned to different phenomena, such as spillover of hydrogen, strongly chemisorbed hydrogen or hydrogen in subsurface layers of the platinum and oxidation of the reduced metal by protons from the supporting material.

The desorption of hydrogen on Pt or Ni supported catalysts at high temperatures was observed by Kramer and Andre [11]. The authors claimed the existence of hydrogen spillover. On the other hand, Rochefort et al. [12] attributed the desorption peak around 773 K to the hydrogen strongly adsorbed on very small dispersed platinum particles supported on α-Al_2O_3.

With the addition of a second metal only one H_2 desorption peak at higher temperatures was observed, which according to the literature, suggests a strong interaction between hydrogen and the active sites. The presence of a single desorption peak on these systems is related to a decrease in the number of bonding sites, associated with a poor dispersion of the metal.

The Pt/MoO_3 catalysts in the presence of H_2 produce H_xMoO_3 bronzes due to the hydrogen spillover, according to Hoang-Van and Zegaoui [7]. The values of x (H_xMoO_3) for various temperatures were obtained from volumetric H_2 consumption measurements, assuming that these bronzes were the only species formed. Based on these results the authors concluded that the bronze composition is directly related to the employed reduction temperature.

Table 1 presents the amount of desorbed hydrogen for tested catalysts.

It shows that the amount of desorbed hydrogen increases with increasing Mo loading for the catalysts containing <14 wt.%. However, for 1Pt20Mo catalyst the amount of H_2 desorbed is less than that for

Table 1
Amount of desorbed H_2 during H_2 TPD

Catalyst	H_2 desorbed (μmol/g catalyst)
1 Pt	2.1
1Pt2Mo	19.6
1Pt8Mo	32.4
1Pt14Mo	44.8
1Pt20Mo	12.8

Table 2
Amount of desorbed H_2 for 1Pt20Mo catalyst

Catalyst	H_2 desorbed (μmol/g catalyst)
1Pt20Mo (blank)	12.1
1Pt20Mo	12.4

1Pt14Mo catalyst. The difference is that for Mo content lower than 14 wt.%, the Mo species are very well dispersed on alumina and hence the Pt dispersion too, which probably favor the spillover of H_2 from Pt to Mo species and, as a consequence, easier bronze formation at lower temperature. On the other hand, for 1Pt20Mo catalyst there are large Mo particles in addition to dispersed Mo phases and, therefore, the dispersion of platinum particles is lower than on dispersed Mo phases. This diminishes the contact between Pt and Mo oxide, which indeed prevent spillover of H_2, reducing the adsorption capacity of 1Pt20Mo as observed. This is in agreement with data reported in the literature [4]. In order to establish the origin of this hydrogen, a "blank" experiment was made with the 1Pt20Mo catalyst. The procedure was similar to the H_2 TPD experiment, except for the hydrogen chemisorption step. Table 2 shows the amount of desorbed hydrogen, as well as values from the H_2 TPD. Notice that the amounts of desorbed hydrogen in these experiments are similar, indicating that bronze formation occurs during the reduction step.

3.3. Nitric oxide temperature programmed desorption (NO TPD)

Fig. 4 displays the NO TPD profiles for the 1Pt catalyst reduced at 773 K.

Notice that 1Pt catalyst presents significant NO desorption peaks at 451 and 637 K, one N_2O peak at 423 K, a small peak of N_2 at 489 K and one O_2 desorption peak at 807 K.

Fig. 5 displays the desorption profiles of N_2 for bimetallic catalysts. As Mo loading increases, the amount of N_2 desorption also increases. These results suggest that molybdenum is the main responsible for the NO dissociation to N_2.

The desorption profiles of H_2 during the NO desorption are shown in Fig. 6. All catalysts presented only one peak around 800 K. Interesting is that the

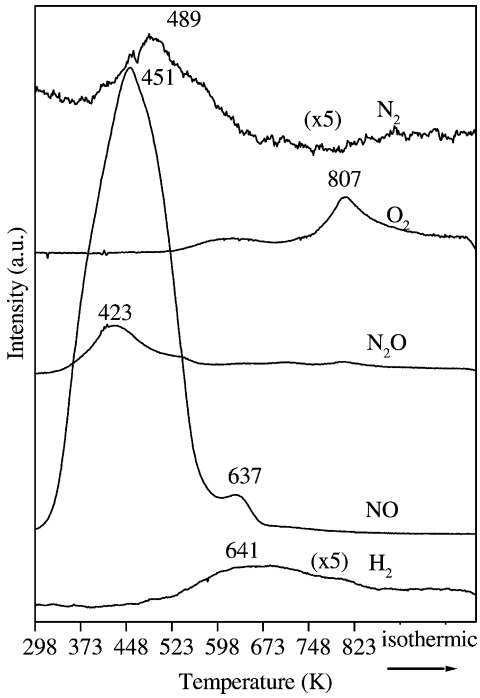

Fig. 4. Desorption profiles, after NO adsorption on 1Pt catalyst reduced at 773 K.

amount of H_2 desorption increases with increasing the Mo content. The significant amount of desorbed H_2 for 1Pt8Mo, 1Pt14Mo and 1Pt20Mo catalysts can be attributed to bronze (H_xMoO_3) decomposition [4,7,11]. These results agree with the TGA/DTA and H_2 TPD data, respectively, predicting the temperature of bronze formation and decomposition and, therefore, the H_2 released corresponds to a back spillover of H_2 during the NO TPD, which is also in agreement with data reported in literature [13].

Table 3 shows the product distribution of nitrogen compounds based on NO TPD profiles. The selectivity

Table 3
Distribution (%) of nitrogen compounds

Catalyst	NO (%)	N_2O (%)	N_2(%)
1Pt	95.3	2.5	2.2
1Pt2Mo	95.8	1.0	3.2
1Pt8Mo	27.5	4.6	67.9
1Pt14Mo	12.2	2.9	84.9
1Pt20Mo	19.3	7.5	73.2

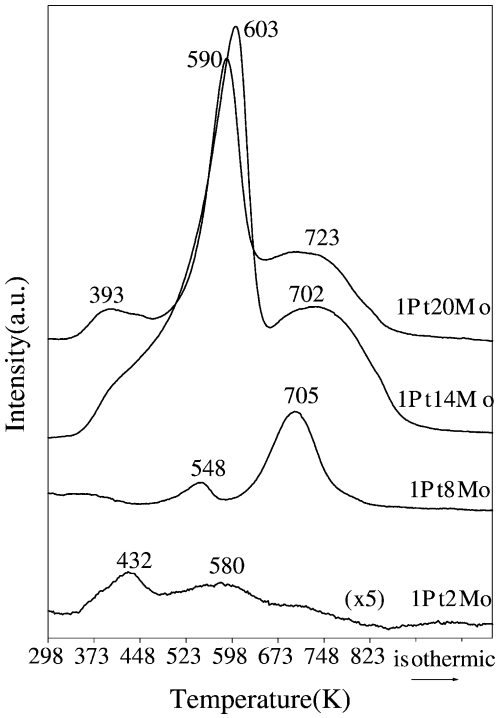

Fig. 5. N_2 profiles for TPD with Pt-MoO_3/γ-Al_2O_3 catalysts reduced at 773 K, after NO adsorption.

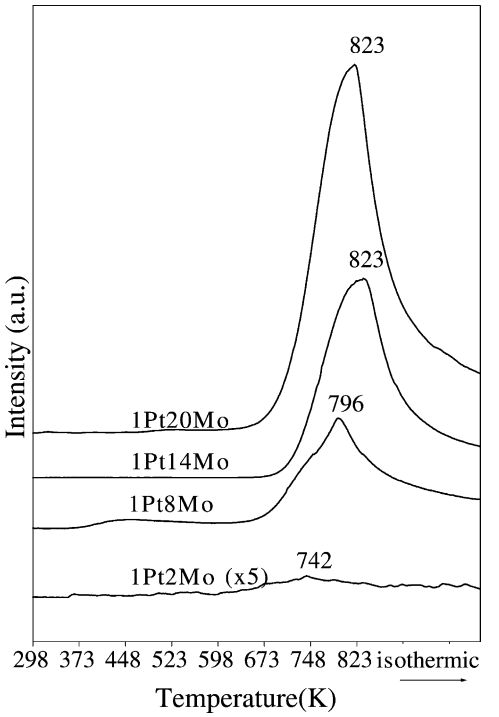

Fig. 6. H_2 profiles for TPD with Pt-MoO_3/γ-Al_2O_3 catalysts reduced at 773 K, after NO adsorption.

towards N_2 increases as the Mo loading increases. In addition, a previous study on NO TPD with 20 wt.% Mo/Al_2O_3 catalyst showed desorption peaks of N_2 and N_2O, that confirm the ability of Mo to dissociate NO [11].

According to the literature [14–16], NO adsorption occurs on partially reduced oxides, such as Pd supported on MoO_3, CeO_2, La_2O_3, which are then re-oxidized after decomposition of NO, releasing N_2. This explanation holds for the catalysts tested in this work. Indeed, during reduction, platinum promotes molybdenum oxide reduction, increasing the availability of molybdenum sites for NO adsorption.

The intriguing question arises from the augmenting amount of H_2 desorption with increasing Mo content, in particular, for 1Pt20Mo sample, during the NO desorption as compared to TPD of H_2 experiment. Besides N_2, N_2O, H_2 and NO desorption we also observed O_2 desorption on all samples but, in particular, on Mo containing samples at lower temperatures. During the NO decomposition the following reaction may occur: $4NO \rightarrow 2N_2O + O_2$. As Mo^{6+} can be reduced during the reduction step with H_2 to a lower oxidation state, according to $2Mo^{6+} + H_2 \rightarrow 2Mo^{\delta+} + [HO]^{\delta-}$ it suggests that the presence of oxygen due to the decomposition of NO re-oxidizes the $Mo^{\delta+}$ and reacts with the OH at the Mo surface (reverse reaction), and decomposes again H_2O in H_2 and O_2, justifying the increasing amount of H_2 during the NO decomposition on Mo containing catalyst. Notice that the H_2 formation on Pt/Al_2O_3 catalyst is too small compared to the containing Pt/Mo catalysts.

3.4. Reduction of NO by CO

Results for NO conversion and N_2 selectivity at 573 K are shown in Table 4. Products, detected by gas chromatography, were N_2, N_2O and CO_2. The catalytic effect of Pt on reaction between CO and NO has been explained by NO dissociation into nitrogen and oxygen [17]. For 1Pt catalyst, N_2 selectivity was 28%. However, in the presence of water the

Table 4
NO conversion and N_2 selectivity for the catalysts at 573 K

Catalyst	Without H_2O		With H_2O		After suppression of H_2O	
	X_{NO}	Selectivity towards N_2 (%)	X_{NO}	Selectivity towards N_2 (%)	X_{NO}	Selectivity towards N_2 (%)
1Pt	2.7	28	52.9	64	19	48
1Pt8Mo	6.2	31	47.5	90	12.4	61
1Pt20Mo	5.5	12	44.6	100	12.1	0

conversion was significantly increased and selectivity of N_2 augmented by a factor of 3 or more with increasing Mo loading. For 1Pt20Mo, selectivity reached the maximum value of 100% at isoconversion, a marked enhance as compared to the reaction without water (12%; Table 4). After suppression of water, the conversion decreased but remains greater than the initial step without water. In contrast, the selectivity of N_2 decreased drastically when compared to Pt/Al_2O_3.

There are two possibilities, which may explain this behavior. Firstly, an oxi-reduction process, similar to the Pd-Mo system, as reported in [14]. This process is envisioned in the following mechanism, which explains the enhancement of N_2 selectivity for Mo catalysts.

$$PtO_2 + 2H_2 \rightarrow Pt^0 + 2H_2O, \quad \text{reduction step}$$

$$2Mo^{6+} + \tfrac{1}{2}\delta H_2 \rightarrow 2Mo^{\delta+} + \delta[HO]^-$$

$$CO + Pt^0 \rightarrow Pt\text{-}CO_{ads}$$

$$2NO + Mo^{\delta+}(Mo^{4+}) \rightarrow N_2 + Mo^{6+}$$

$$Pt^0\text{-}CO_{ads} + Mo^{6+} \rightarrow Mo^{\delta+}(Mo^{4+}) + CO_2 + Pt^0$$

In addition, DRIFT measurements on $Pd8Mo/Al_2O_3$ catalyst as reported in [14] showed that after exposure to NO+CO at 573 K a typical large band appeared near 2231 cm^{-1}, corresponding to an isocyanate complex. [18]. This band did not disappear after purging with Ar and was very stable. It is not attributed to the Al^{3+}–CO formation, as observed on the Pd/Al_2O_3 catalyst, and the intensity of this adsorption band increased during the reaction of NO + CO. It was just attributed to the isocyanate formation.

In addition to NO and N_2O, our results presented CO_2 formation during the reaction in the presence of water or not. It turns out that in the presence of water this isocyanate can be transformed into an intermediate isocyanic acid, which then reacts with water, as follows:

$$–NCO + H_2O \rightarrow CO_2 + HNCO$$

$$HNCO + H_2O \rightarrow CO_2 + NH_3$$

Therefore, water will destroy or prevent the isocyanate formation, which is otherwise stable in the absence of water, enhancing the reduction of Mo at the surface. According to the oxi-reduction process, it increases selectivity toward N_2, in good agreement with results displayed in Table 4. After suppression of water the selectivity decreases just because isocyanate cannot be destroyed, inhibiting the Mo reduction at the surface.

The second possibility is to explain the surface transformation during reaction. Probably due to elimination of residual chlorine from the platinum precursor salt, the Pt^0 number of sites increase. However, water can also modify the surface by forming $Pt^{\delta+}(OH)$ sites, which according to literature, act as inhibitors [19].

The catalytic activity in the absence of water was low, due to surface oxi-chloride species and/or interaction of residual chlorine with metallic sites.

The catalytic activity increased significantly in the presence of water. Dissociation of adsorbed water on Pt^0 gives H^* and OH^* species that can easily recombine, but in the presence of Cl, H^* reacts with Cl at the metallic interface, producing HCl and regenerating the sites according to the reaction:

$$Cl\text{-}Pt^* + H\text{-}Pt^* \rightarrow HCl_{(g)} + 2Pt^*$$

where * represents the metallic site.

The bimetallic catalysts presented similar conversions, independent of Mo loading. However, 1Pt8Mo catalyst was more selective towards N_2 even after the suppression of water. Similar results were obtained by Gandhi et al. [3].

These results suggest the existence of three types of sites: Pt, $Mo^{\delta+}$ and $PtMo^{\delta+}$, this later one at the interface of platinum-molybdenum partially reduced. The promoting effect of Mo can be related to a mechanism, where NO is preferentially adsorbed on partially reduced Mo sites releasing N_2, while CO is adsorbed predominantly on platinum sites releasing CO_2. Indeed, these catalysts presented lower dispersion than 1Pt catalyst [4], which can be explained by Pt encapsulation via partially reduced Mo species [4,20,21]. However, the addition of water decreased the encapsulation of platinum sites increasing the number of Pt and Pt-$Mo^{\delta+}$ sites, which are more selective for the N_2 formation. Worthy noting the distinguished behavior of 1Pt8Mo and 1Pt20Mo catalysts, regarding the suppression of water: the first exhibited more Pt-$Mo^{\delta+}$ and Pt sites while the second did not form N_2. Indeed, with 20% Mo loading, only MoO_3 crystals have been observed [4]. Therefore, the catalytic performance can be accounted for in terms of the surface reaction conditions that transformed markedly the surface properties of the catalysts, by changing the types of the active sites as well as the accessibility.

4. Conclusions

The thermal analysis and H_2 desorption results proof bronze formation during the reduction of Pt oxide in the presence of Mo oxide coated on alumina support.

The NO TPD results indicate that Mo is responsible for higher N_2 selectivity on the bimetallic catalysts (Mo $\geq$8%). They are also consistent with formation of bronze species (H_xMoO_3) for catalysts with high Mo content, in agreement with other characterization techniques. The reaction between NO and CO suggest the existence of synergy between Pt and Mo, in which platinum maintains the surrounding molybdenum particles in its more active form.

Product selectivity of the NO reduction by CO is function of the prevailing treatment and reaction conditions and suggests significant changes of surface sites during the reaction.

Acknowledgements

The authors acknowledge the CNPq for financial support.

References

[1] I. Halasz, A. Brenner, M. Shelef, K.Y. Simon Ng, Appl. Catal. A 82 (1992) 51.
[2] I. Halasz, A. Brenner, M. Shelef, Appl. Catal. B 2 (1993) 131.
[3] H.S. Gandhi, H.C. Yao, H.K. Stepien, Catalysis under transient conditions, ACS Symp. Ser. No. 178 (1982) 143.
[4] M.A.P. Silva, R.A.M. Vieira, M. Schmal, Appl. Catal. A 190 (2000) 170.
[5] M.A.P. Silva, R.A.M. Vieira, M. Schmal, in: Proceedings of the Actas do XVth Simpósio Iberoamericano de Catalisis, vol. 2, Córdoba, Argentina, 1996, p. 1073.
[6] M.A.S. Baldanza, G.S. Amorin, M.A.P. Silva, M. Schmal, in: Proceedings of the Anais do Eighth Seminário Brasileiro de Catálise, vol. 1, Nova Friburgo, RJ, 1995, p. 212.;
M.A.P. Silva, R.A.M. Vieira, M. Schmal, Appl. Catal. A 190 (2000) 170.
[7] C. Hoang-Van, O. Zegaoui, Appl. Catal. A 130 (1995) 89.
[8] J.T. Miller, B.L. Meyers, F.S. Modica, G.S. Lane, M. Vaarkamp, D.C. Koningsberger, J. Catal. 143 (1993) 395.
[9] J.T. Miller, B.L. Meyers, M.K. Barr, F.S. Modica, D.C. Koningsberger, J. Catal. 159 (1996) 41.
[10] M. Vaarkamp, J.T. Miller, F.S. Modica, D.C. Koningsberger, J. Catal. 163 (1996) 294.
[11] R. Kramer, M. Andre, J. Catal. 58 (1979) 287.
[12] A. Rochefort, F. Le Peltier, J.P. Boitiaux, J. Catal. 138 (1992) 482.
[13] R.L. Martins, M.M.V.M. Souza, D.A.G. Aranda, Stud. Surf. Sci. Catal. 138 (2001) 77.
[14] M. Schmal, M.A.S. Baldanza, M. Albert Vannice, J. Catal. 185 (1999) 138.
[15] H. Cordatos, R.J. Gorte, J. Catal. 159 (1996) 112.
[16] M. Valden, R.L. Keiski, N. Xiang, J. Pere, J. Aaltonen, M. Pessa, T. Maunula, A. Savimaki, A. Lahti, M. Harkonen, J. Catal. 161 (1996) 614.
[17] E.W. Scharpf, J.B. Benziger, J. Catal. 136 (1992) 342.
[18] R. Dompelmann, N.W. Cant, D.L. Trimm, Appl. Catal. B 6 (1995) L291.
[19] M. Schmal, D.A.G. Aranda, F.B. Noronha, A.L. Guimarães, R.S. Monteiro, Catal. Lett. 64 (2000) 163.
[20] G. Leclercq, A.El. Gharbi, L. Gengembre, T. Romero, L. Leclercq, S. Pietrzyk, J. Catal. 148 (1994) 550.
[21] S.H. Choi, J.S. Lee, J. Catal. 167 (1997) 364.